AD-A225 561

RADC-TR-89-237
In-House Report
October 1989

DTIC FILE COPY

A PRINTED CIRCUIT FOLDED DIPOLE WITH INTEGRATED BALUN

Paul M. Proudfoot, 1/Lt, USAF

APPROVED FOR PUBLIC RELEASE; DISTRIBUTION UNLIMITED.

ROME AIR DEVELOPMENT CENTER
Air Force Systems Command
Griffiss Air Force Base, NY 13441-5700

055

This report has been reviewed by the RADC Public Affairs Office (PA) and is releasable to the National Technical Information Service (NTIS). At NTIS it will be releasable to the general public, including foreign nations.

RADC TR-89-237 has been reviewed and is approved for publication.

APPROVED:

ROBERT J. MAILLOUX, Chief
Antennas and Components Division
Directorate of Electromagnetics

APPROVED:

JOHN K. SCHINDLER
Director of Electromagnetics

FOR THE COMMANDER:

JOHN A. RITZ
Directorate of Plans and Programs

If your address has changed or if you wish to be removed from the RADC mailing list, or if the addressee is no longer employed by your organization, please notify RADC (EEAA) Hanscom AFB MA 01731-5000. This will assist us in maintaining a current mailing list.

Do not return copies of this report unless contractual obligations or notices on a specific document requires that it be returned.

REPORT DOCUMENTATION PAGE

Form Approved
OMB No. 0704-0188

Public reporting for this collection of information is estimated to average 1 hour per response, including the time for reviewing instructions, searching existing data sources, gathering and maintaining the data needed, and completing and reviewing the collection of information. Send comments regarding this burden estimate or any other aspect of this collection of information, including suggestions for reducing this burden, to Washington Headquarters Services, Directorate for Information Operations and Reports, 1215 Jefferson Davis Highway, Suite 1204, Arlington, VA 22202-4302, and to the Office of Management and Budget, Paperwork Reduction Project (0704-0188), Washington, DC 20503.

1. AGENCY USE ONLY (Leave blank)	2. REPORT DATE	3. REPORT TYPE AND DATES COVERED
	Oct 89	In-House Jun 88 - Mar 89

4. TITLE AND SUBTITLE
A Printed Circuit Folded Dipole with Integrated Balun

5. FUNDING NUMBERS
PE 61102F
PR 2305
TA J3
WU 03

6. AUTHOR(S)
Proudfoot, Paul M., 1Lt, USAF

7. PERFORMING ORGANIZATION NAME(S) AND ADDRESS(ES)
Rome Air Development Center
RADC/EEAA
Hanscom AFB
Massachusetts 01731-5000

8. PERFORMING ORGANIZATION REPORT NUMBER
RADC-TR-89-237

9. SPONSORING/MONITORING AGENCY NAME(S) AND ADDRESS(ES)

10. SPONSORING/MONITORING AGENCY REPORT NUMBER

11. SUPPLEMENTARY NOTES

12a. DISTRIBUTION/AVAILABILITY STATEMENT
Approved for public release; distribution unlimited.

12b. DISTRIBUTION CODE

13. ABSTRACT (Maximum 200 words)

This report documents the design and testing of a printed circuit folded dipole with a unique double-tuning balun as feed. Simple transmission line theory is used to analyze the balun structure, whereas the method-of-moments and conformal mapping techniques are used to analyze the dipole impedance and step-up ratio. Two dipoles were then fabricated on substrates of different dielectric constant material. The antenna designs were then tested for impedence match and radiation characteristics. First, SWR measurements were made on the two dipoles that were fabricated, and the results compared to theory. Next, antenna patterns are taken of the folded dipoles at several frequencies over the operating band to determine any frequency dependence of the patterns. Finally, cross-polarization patterns are presented.

14. SUBJECT TERMS		15. NUMBER OF PAGES
Folded Dipole Balun	Printed Circuit Antennas	44
		16. PRICE CODE

17. SECURITY CLASSIFICATION OF REPORT	18. SECURITY CLASSIFICATION OF THIS PAGE	19. SECURITY CLASSIFICATION OF ABSTRACT	20. LIMITATION OF ABSTRACT
UNCLASSIFIED	UNCLASSIFIED	UNCLASSIFIED	SAR

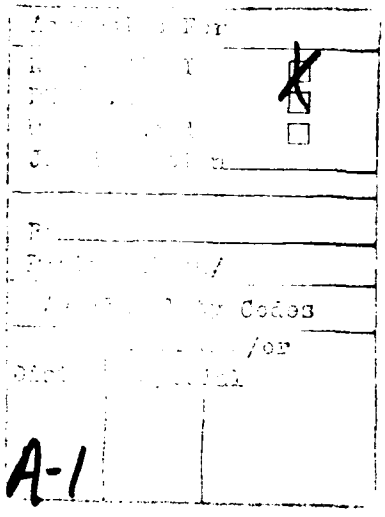

Contents

1. INTRODUCTION 1

2. MODEL 3

   2.1 The Balun 3
   2.2 The Dipole 10

3. RESULTS 16

   3.1 Dipole Fabrication 16
   3.2 VSWR Measurements 18
   3.3 Antenna Patterns 21

4. CONCLUSION 36

REFERENCES 37

Illustrations

1.	Conventional Dipole with Integrated Balun	2
2.	Folded Dipole with Integrated Balun	4
3.	Coaxial Equivalent Circuit	4
4.	Fields Beneath a Microstrip Line	9
5.	Folded Dipole Geometry	10
6.	Modes of Operation	11
7.	Dipole Equivalent Circuit	12
8.	Input Impedance of a Dipole	15
9.	Folded Dipole over a Ground Plane	17
10.	Measured and Theoretical VSWR, 4.4 Material	19
11.	Measured and Theoretical VSWR, 2.54 Material	20
12.	Antenna Patterns, 4.4 Material, 3.7 GHz: a) E-Plane b) H-Plane	22
13.	Antenna Patterns, 2.54 Material, 4.2 GHz: a) E-Plane b) H-Plane	23
14.	Antenna Patterns, 4.4 Material, 3.1 GHz: a) E-Plane b) H-Plane	25
15.	Antenna Patterns, 4.4 Material, 4.2 GHz: a) E-Plane b) H-Plane	26
16.	Antenna Patterns, 2.54 Material, 3.5 GHz: a) E-Plane b) H-Plane	27
17.	Antenna Patterns, 2.54 Material, 5.0 GHz: a) E-Plane b) H-Plane	28

18. Cross-Polarized Patterns, 4.4 Material, 3.1 GHz: a) E-Plane b) H-Plane 30
19. Cross-Polarized Patterns, 4.4 Material, 3.7 GHz: a) E-Plane b) H-Plane 31
20. Cross-Polarized Patterns, 4.4 Material, 4.2 GHz: a) E-Plane b) H-Plane 32
21. Cross-Polarized Patterns, 2.54 Material, 3.5 GHz: a) E-Plane b) H-Plane 33
22. Cross-Polarized Patterns, 2.54 Material, 4.2 GHz: a) E-Plane b) H-Plane 34
23. Cross-Polarized Patterns, 2.54 Material, 5.0 GHz: a) E-Plane b) H-Plane 35

A Printed Circuit Folded Dipole with Integrated Balun

1. INTRODUCTION

To date, printed folded dipoles have been developed empirically. One paper[1] gives equations for the design of a printed folded dipole, but no measured results are presented. This report documents the design and testing of such a printed circuit folded dipole. The folded dipole is an appealing choice as a radiating element because its input impedance can be made to match that of a printed circuit transmission line over a four-to-one range (typically 70-280 ohms).

Printed folded dipoles are typically fed using an equal split power divider with an 180 degree phase shift in one arm.[2] This report presents a unique combination of a folded dipole with a printed-circuit double-tuning balun as feed. Feeding the dipole in this manner allows us to combine the moderate bandwidth of the folded dipole with the double tuning capability of the balun to produce an element with significantly greater bandwidth than conventional

---

(Received for Publication 3 Nov 1989)

[1] Lampe, R.L. (1985) Design formulas for an asymmetric coplanar strip folded dipole, *IEEE Trans. Antennas Propagat.* AP-33:1023-1031.

[2] Herper, J.C., Hessel, A., and Tomasic, B. (1985) Element pattern of an axial dipole in a cylindrical phased array, Part II, *IEEE Trans. Antennas Propagat.* AP-33:273-278.

patch radiators. Because the dipole/balun configuration is a printed circuit element, it has the important advantages of being a low-cost and light-weight device.

A conventional printed dipole with integrated balun[3] is shown in Figure 1. In this configuration, the input impedance of the dipole (usually 75-80 ohms) dictates the widths of the microstrip and coupled microstrip lines that make up the balun. However, a problem that can arise in the design of a dipole on a particular substrate is that the coupled microstrip lines can become wider than the length of the dipole arms. The folded dipole alleviates this problem in that its higher impedance is matched by a feed line of reduced width. Now, a dipole element that could not be fabricated on a particular substrate due to excessive coupled microstrip line widths becomes feasible.

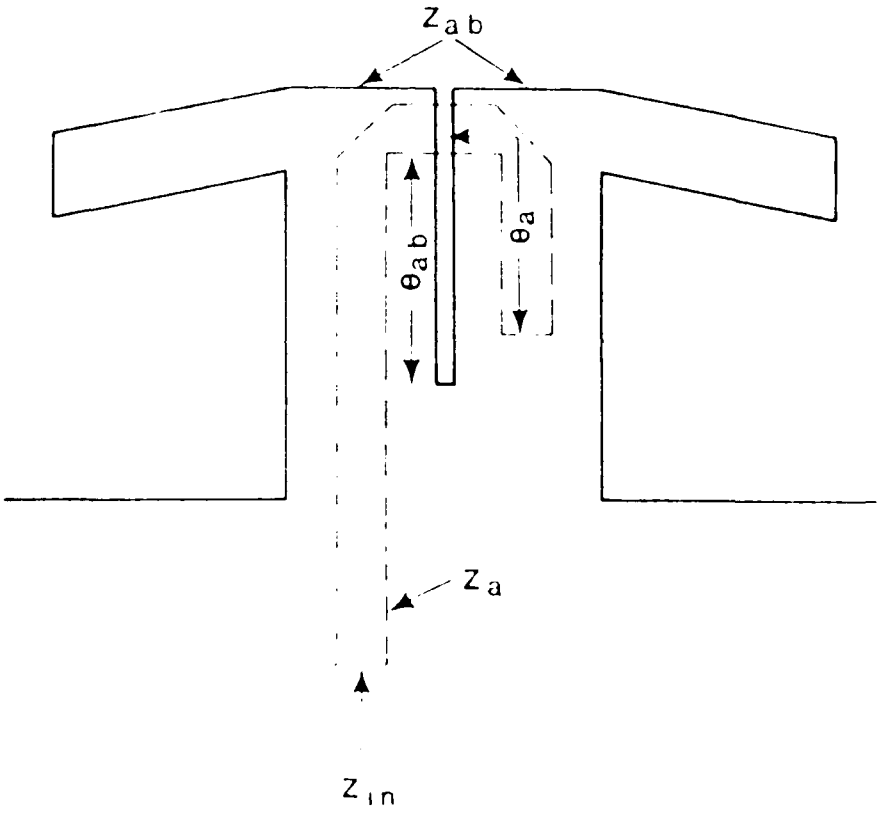

Figure 1. Conventional Dipole with Integrated Balun

[3] Edward, B. and Rees, D. (1987) A broadband printed dipole with integrated balun, *Microwave J.* **30**:339-344.

Simple transmission line theory is used to analyze the balun structure, whereas the method-of-moments and conformal mapping techniques are used to analyze the dipole impedance and step-up ratio.

The printed folded dipole also is in the class of endfire radiators (that is the dipole radiates in the plane of the substrate). Endfire radiators are relatively easy to array, in that all feed lines and active devices are located behind the antenna element. Here, they won't interfere with tight interelement spacings. Also, a metal ground plane shields the antenna half-space from spurious radiation emitted by feed lines and active devices. This will prevent degradation of sidelobe levels, polarization, and gain in an array environment.

To demonstrate the broadband operation of the folded dipole/balun configuration, two dipoles were fabricated on substrates of different dielectric constant material. The antenna designs were then tested for impedance match and radiation characteristics. First, SWR measurements are made on the two dipoles that were fabricated, and the results compared to theory. Next, antenna patterns are taken of the folded dipoles at several frequencies over the operating band to determine any frequency dependence of the patterns. Finally, cross-polarization patterns are presented.

2. MODEL

2.1 The Balun

The key to the wide-band operation of the dipole/balun configuration is the double-tuning capability of the balun. The wide-band balun used in this experiment was first proposed by Roberts[4] was later put into printed circuit form by Bawer and Wolfe[5] and was most recently used by Edward and Rees[3] in a similar experiment. Figure 2 illustrates the geometry of the printed circuit dipole/balun. The coaxial equivalent[2] to the printed circuit is shown in Figure 3.

---

[4] Roberts, W.K. (1957) A new wide-band balun, *Proc. IRE* 45:1628-1631.

[5] Bawer, R. and Wolfe, J.J. (1960) A printed circuit balun for use with spiral antennas, *IRE Trans. on Microwave Theory Tech.* MTT-8:319-325.

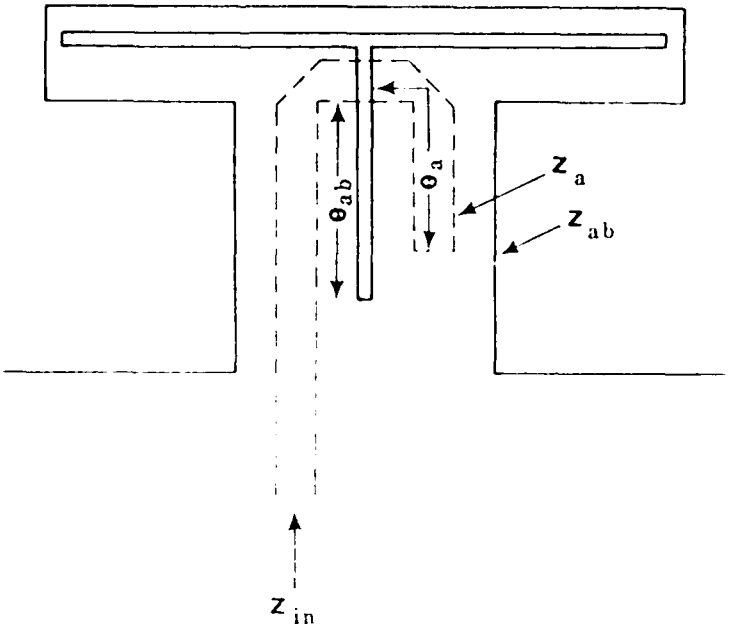

Figure 2. Folded Dipole with Integrated Balun

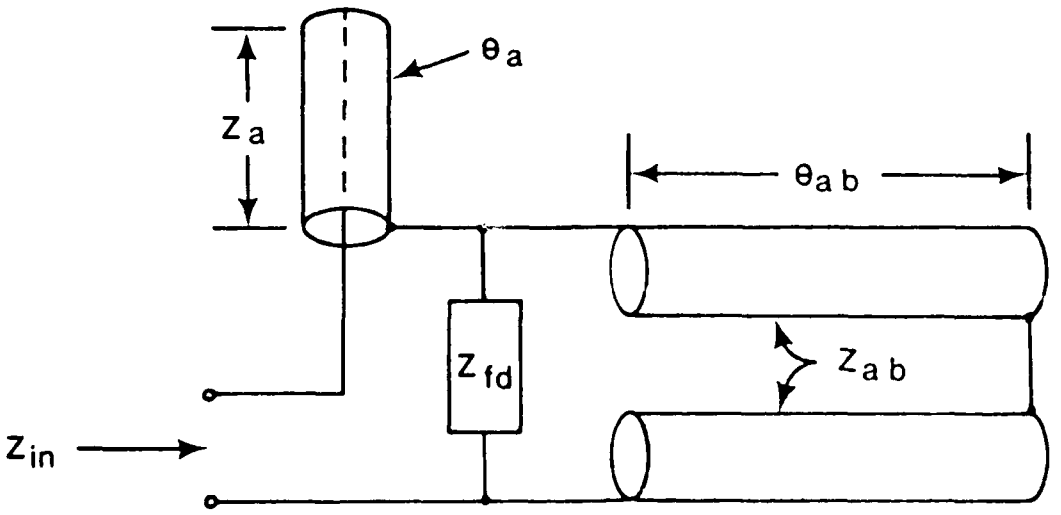

Figure 3. Coaxial Equivalent Circuit

In the coaxial circuit, the folded dipole input impedance is simply represented by a complex value Z_{fd}. By inspection of the circuit in Figure 3, the input impedance Z_{in} can be expressed as:

$$Z_{in} = -j\, Z_a \cot \theta_a + \frac{j\, Z_{fd}\, Z_{ab} \tan \theta_{ab}}{Z_{fd} + j\, Z_{ab} \tan \theta_{ab}} \qquad (1)$$

where Z_a, θ_a, Z_{ab}, and θ_{ab} are the characteristic impedance and electrical length of the microstrip and coupled microstrip lines respectively. By judicious selection of the parameters θ_a and θ_{ab} (that is, the open-end length and slot length) in Eq. (1), one can achieve an impedance match over a very wide bandwidth. The rest of this section is devoted to determining the balun parameters Z_a, θ_a, Z_{ab}, and θ_{ab}.

The characteristic impedance Z_a of a microstrip line of width W, on a substrate thickness h and dielectric constant ε_r, and foil thickness t is[6]:

$$Z_a = \begin{cases} \dfrac{\eta}{2\pi\sqrt{\varepsilon_r}} \ln\left[\dfrac{8h}{W_e} + .025\dfrac{W_e}{h}\right] & \dfrac{W}{h} \le 1 \\ \dfrac{\eta}{\sqrt{\varepsilon_r}}\left[\dfrac{W_e}{h} + 1.393 + .667 \ln\left(\dfrac{W_e}{h} + 1.444\right)\right]^{-1} & \dfrac{W}{h} > 1 \end{cases} \qquad (2)$$

where η is the impedance of free space, 120π. W_e is the effective line width, which accounts for fringing fields near the strip edge.

$$W_e = W + 1.25\,\frac{t\,\delta}{\pi}$$

---

[6] Gupta, K.C., Garg, R., and Chadha, R. (1981) *Computer Aided Design of Microwave Circuits*, Artech House, Dedham, MA.

$$\delta = \begin{cases} 1 + \ln(4\pi W/t) & \dfrac{W}{h} \leq \dfrac{1}{2\pi} \\ 1 + \ln(2h / t) & \dfrac{W}{h} > \dfrac{1}{2\pi} \end{cases} \tag{3}$$

A FORTRAN subroutine that calculates the correct microstrip width for a given impedance and substrate, can be found in RADC-TM-86-08.[7]

When calculating the electrical length θ_a and characteristic impedance Z_a of the microstrip line, the effective dielectric constant

$$\varepsilon_{eff} = \frac{\varepsilon_r + 1}{2} + \frac{\varepsilon_r - 1}{2}\left[1 + \frac{10h}{W}\right]^{-1/2} - \frac{\varepsilon_r - 1}{4.6}\frac{t/h}{\sqrt{W/h}} \tag{4}$$

is used.

The electrical length θ_a is then:

$$\theta_a = \frac{2\pi}{\lambda_\varepsilon} l_a \tag{5}$$

where

$$\lambda_a = \frac{\lambda_o}{\sqrt{\varepsilon_{eff}}}$$

and λ_o is the free space wavelength. The physical l_a of the microstrip line is measured starting at the mid-point between the two coupled microstrip lines (see Figure 2), runs

---

[7] McGrath, D.T., Mullinix, D.A., and Huck, K.D. (1986) *FORTRAN Subroutines for Design of Printed Circuit Antennas*, RADC-TM-86-08, ADB107263L.

along the inside edge of the mitered bend, and terminates at the open end. The length extension:[6]

$$\Delta l = .412h \frac{(\varepsilon_{eff} + 0.3)}{(\varepsilon_{eff} - 0.258)} \frac{(W/h + 0.264)}{(W/h + 0.8)} \quad (6)$$

is then added to l_a to account for fringing fields that occur at the open-end discontinuity.

Values for Z_{ab} and θ_{ab} are determined using the odd-mode characteristic impedance and effective dielectric constant of a coupled microstrip line. There are several good references in which these equations can be found.[6,8,9] One reference in particular[9] gave closed form, easy-to-use equations that are accurate even into the millimeter-wave region. The physical length used in determining θ_{ab} is measured from the lower edge of the microstrip line (see Figure 2) to the bottom of the slot.

Selecting a suitable substrate for the folded dipole is not as critical as selecting a substrate for the conventional dipole like the one shown in Figure 1. Once a substrate is selected for the conventional dipole, the designer has very little freedom to vary microstrip and coupled microstrip line widths, whereas, with the folded dipole the designer can choose a microstrip line impedance anywhere from 70 to 280 ohms. In both the conventional and folded dipole cases, the balun works the same way, the only difference being the higher Z_a, Z_{ab} and Z_{fd} impedance values for the folded dipole.

In the balun structure, the coupled microstrip line acts as ground plane to the microstrip line (see Figure 4). Note in this figure, that virtually all of the fields beneath the microstrip line of width W are contained within 3W.[4] Therefore, the width of the coupled microstrip line must be greater than 3W. Since there are two coupled microstrip lines, the dimension B (in Figure 4) must be greater than 6W. For the conventional dipole, this transverse dimension B is now a major limitation to both the upper value of Z_{ab} and to the maximum frequency for which a dipole can be fabricated on a particular substrate. For example, the dipole length (L) is approximately 0.43λ, or 0.42 in. at 12 GHz. The material available for dipole fabrication is 1/16 in. thick substrate with dielectric

---

[8] Akhtarzad, S., Rowbotham, T.R., and Johns, P.B. (1975) The design of coupled microstrip lines, *IEEE Trans. Microwave Theory Tech.* MTT-23:486-492.

[9] Kirschning, M. and Jansen, R.H. (1984) Accurate wide-range design equations for the frequency dependent characteristics of parallel coupled microstrip lines, *IEEE Trans. Microwave Theory Tech.* MTT-32:83-90.

constant 2.2. The 80 ohm line required to feed the conventional dipole is 0.085 in. wide. Dimension B is 6 times this line width or 0.51 in. Hence, a 12 GHz conventional dipole could not be fabricated using this substrate. A folded dipole however, could be used. The 120 ohm (higher if needed) line required to feed a folded dipole is 0.034 in. wide. The dimension B is therefore 0.2 in., or less than half of the length of the dipole arms. To keep all dipole/balun dimensions in proportion, it is suggested that $0.4L < B < 0.5L$. Finally, a substrate should be selected that is electrically thin ($h/\lambda_\varepsilon < 0.1$). This constraint will help insure that the equations used in determining Z_a, θ_a, Z_{ab}, and θ_{ab} will yield accurate results.

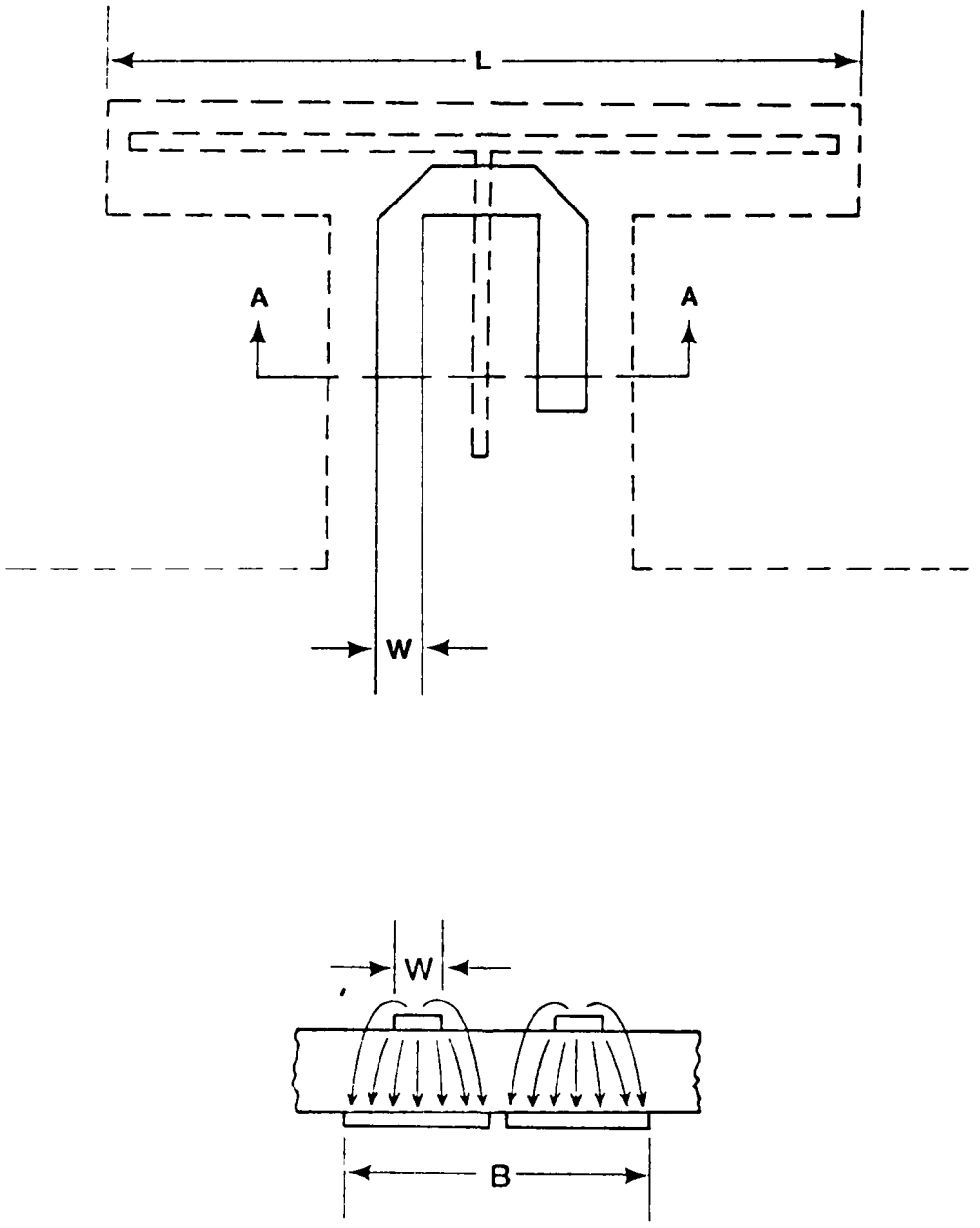

Figure 4. Fields Beneath a Microstrip Line

2.2 The Dipole

A folded dipole like the one shown in Figure 5 is just an extension of the conventional single wire dipole. However, since the folded dipole arms are made up of asymmetric coplanar strips, both the even and odd mode currents must be considered.

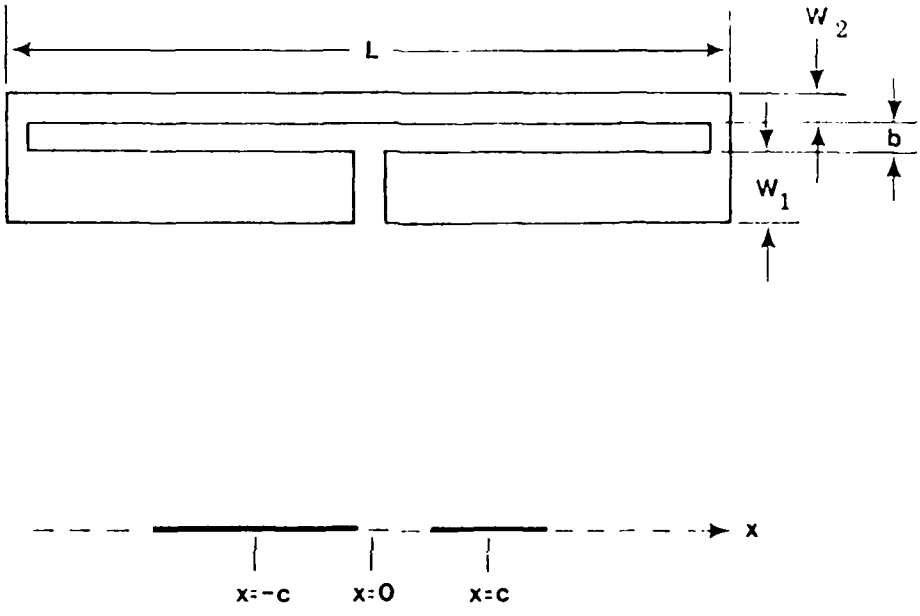

Figure 5. Folded Dipole Geometry

A diagram representing the two modes of operation is shown in Figure 6. In the odd mode, equal currents in the dipole arms travel in opposite directions, resulting in fields that are out of phase and thus cancel in the far field of the antenna. This mode is referred to as the non-radiating (or transmission line) mode. In the even mode, currents in the dipole arms travel in the same direction. The fields generated by these currents add up in-phase, resulting in a radiating (or antenna) mode. By considering currents in the antenna and transmission line modes separately we can solve for the dipole and transmission line currents individually and then superimpose the two currents to find the total input current.[10] Note in Figure 6, that when the two modes are superimposed the voltages in the right arm add up to zero, as they should.

---

[10] Johnson, R.C. and Jasik, H. (1984) *Antenna Engineering Handbook*, McGraw-Hill, New York.

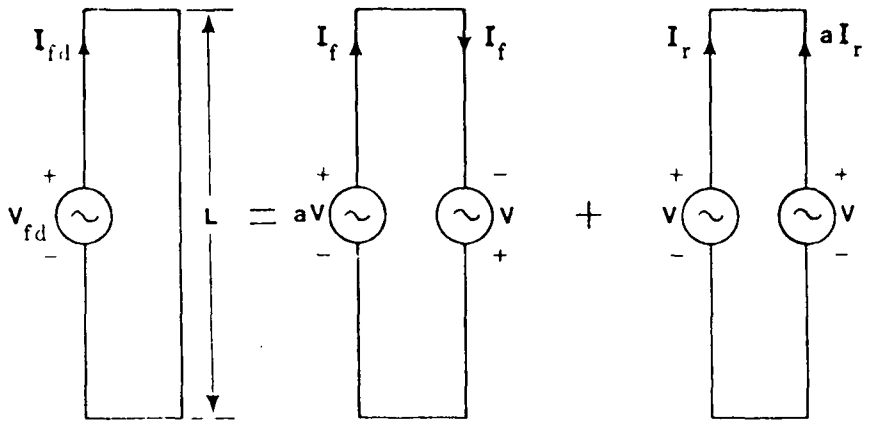

Figure 6. Modes of Operation

A circuit diagram showing how the dipole currents and voltages are related is shown in Figure 7. Here the $2Z_f$ comes from the fact that current I_f passes through two lengths of transmission line each of impedance Z_f and length L/2. The impedance looking into terminal a,b is then:

$$Z_{fd} = \frac{V_{fd}}{I_{fd}} \quad . \tag{7}$$

For the ideal transformer in Figure 7, the currents and voltages are related by the equations:

$$I = \frac{I_r}{(1+a)} \tag{8}$$

and

$$V_{fd} = (1+a)V \quad . \tag{9}$$

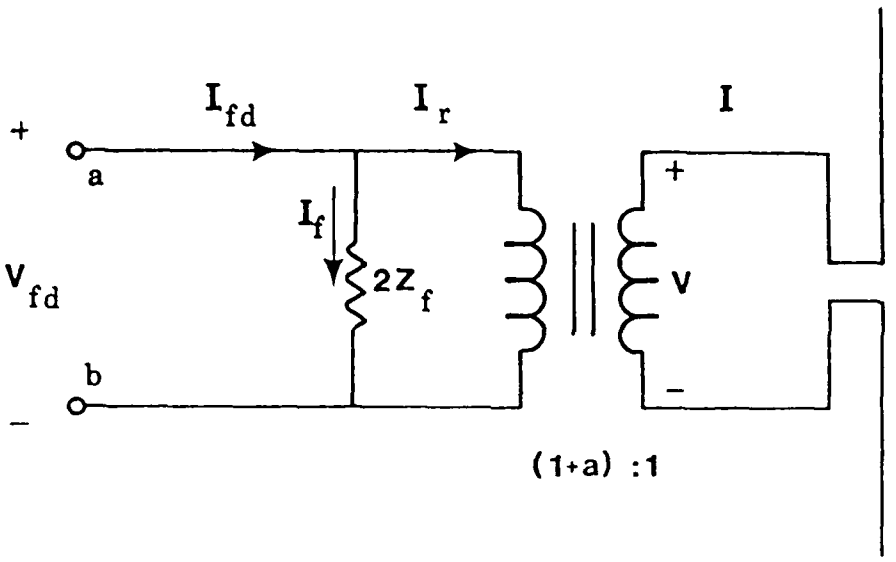

Figure 7. Dipole Equivalent Circuit

We can also write equations for the antenna and transmission line impedances:

$$Z_f = \frac{(1+a)V}{2I_f} \tag{10}$$

and

$$Z_r = \frac{V}{(1+a)I_r} \quad . \tag{11}$$

Substituting Eq. (11) into Eq. (8), Eq. (10) into Eq. (9), and Eqs. (8) and (9) into Eq. (7), we get the input impedance for the folded dipole:

$$Z_{fd} = \frac{2(1+a)^2 Z_d Z_x}{(1+a)^2 Z_d + 2Z_x} \tag{12}$$

where

Z_d = impedance of an equivalent dipole

Z_x = impedance of transmission line

$(1+a)^2$ = impedance step-up ratio.

The transmission line impedance Z_x is that of a shorted transmission line of length L/2, which is given by:

$$Z_x = jZ_o \tan k_o \frac{L}{2} \tag{13}$$

where Z_o is the characteristic of asymmetric coplanar strips and k_o is the wave number. Calculating the characteristic impedance of coplanar strips is similar to the impedance calculation of coplanar slots, which has been solved by conformal mapping techniques,[11] the only difference being that the slots are replaced by conductors, and the conductors are replaced by slots. The results are found to be:

$$Z_o = \frac{120\pi}{\sqrt{\varepsilon_{eff}}} \frac{K(k)}{K'(k)} \tag{14}$$

where ε_r is the dielectric constant of the substrate. $K(k)$ is the complete elliptic integral of the first kind with mutual dependence $K'(k)=K(SQRT(1-k^2))$. Lampe[1] gives the following relationship between the parameter k and the physical dimensions of coplanar strips.

$$k = \frac{b/2[1+e(b/2+W_1)]}{b/2+W_1+e(b/2)^2} \tag{15}$$

---

[11] Hilberg, W. (1969) From approximations to exact relations for characteristic impedances, *IEEE Trans. Microwave Theory Tech.* MTT-17:259-265.

where W_1, W_2 and b are given in Figure 5. Note that if W_1 equals W_2 then the parameter k reduces to the well known result:[6]

$$k = \frac{b}{b+2W}. \tag{16}$$

The impedance step-up ratio $(1+a)^2$ is one of the more attractive features of the folded dipole, as the dipole's input impedance can be varied over a 4:1 range (typically from 70Ω to 280Ω). The term (a) in the impedance step-up ratio is the ratio of currents or charge on the two conductors in the antenna mode. An approximate solution for (a) is given as:[1]

$$a = \frac{Q_2}{Q_1} = \frac{I_2}{I_1} = \frac{\ln(4c+2[(2c)^2-(W_1/2)^2]^{1/2})-\ln(W_1)}{\ln(4c+2[(2c)^2-(W_2/2)^2]^{1/2})-\ln(W_2)} \tag{17}$$

where W_1,$W_2$and c are as in Figure 5.

The last parameter to be determined in Eq (12) is the dipole impedance (Z_d). The impedance of a folded dipole is related to the impedance of an ordinary dipole through the use of an equivalent radius (ρ_e). This equivalent radius is defined by the invariance of capacitance per unit length[12] and given by:

$$\ln(\rho_e) = \frac{Q_1}{Q_1+Q_2}\ln(W_1/4)+\frac{Q_2}{Q_1+Q_2}\ln(c+[c^2-(W_2/4)^2]^{1/2}) \tag{18}$$

If W_1 equals W_2, Eq. (12) reduces to:

$$\rho_e = [(W/4)(c+[c^2-(W/4)^2]^{1/2})]^{1/2}. \tag{19}$$

Equation (19) can be further simplified if W_1 and W_2 are small compared to $2c$, in which case Eq. (19) reduces to:[12]

$$\rho_e = (Wc/2)^{1/2} \tag{20}$$

Balanis[13] presents a computer program, written in FORTRAN, that uses the method-of-moments to determine the input impedance of a dipole for a given dipole length and radius. Figure 8 shows a typical dipole input impedance as calculated with this program.

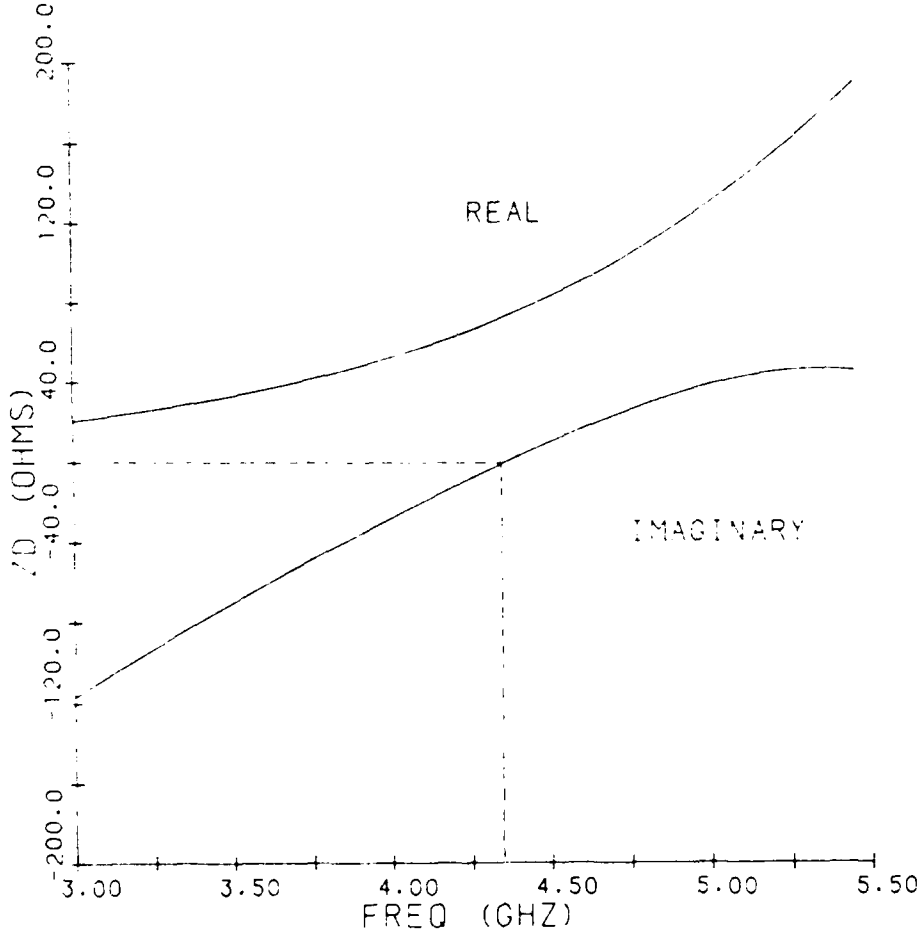

Figure 8. Input Impedance of a Dipole

[12] Lo, Y.T. (1953) A note on the cylindrical antenna of noncircular cross-section, *J. Appl. Phys.*, **24**:1338-1339.

[13] Balanis, C.A. (1982) *Antenna Theory*, Harper and Row, New York, pp. 319-321.

3. RESULTS

3.1 Dipole Fabrication

To demonstrate the broadband operation of the folded dipole/balun configuration, two dipoles were fabricated on 1/16 in. thick substrate. One dipole was etched on a PTFE substrate with dielectric constant 2.54. The other dipole was etched on an epoxy/fiberglass substrate with dielectric constant 4.4. Figure 9 shows one of the dipoles mounted $\lambda_o/4$ above a 16 x 16 in. ground plane. Both dipoles have an arm width of 0.21 in. and a total arm length of 1.2 in. A length extension, equal to 1/2 of a dipole arm width, was added to L to account for radiation effects from the ends of the dipole. Rather than selecting dipole dimensions that would yield an optimum bandwidth for one particular substrate, dimensions were selected such that a good impedance match could be achieved on both substrates. Therefore, even though the 31-36 percent bandwidth achieved by the two dipoles was good, bandwidths of 40 percent are possible.

Both dipoles have an input impedance of about 80Ω at resonance (that is, the dipole and balun impedance combined), therefore, a 80Ω microstrip line is used to feed them. A 62Ω quarter-wave transformer is then utilized to match the microstrip line to a 50Ω jack-tab connector.

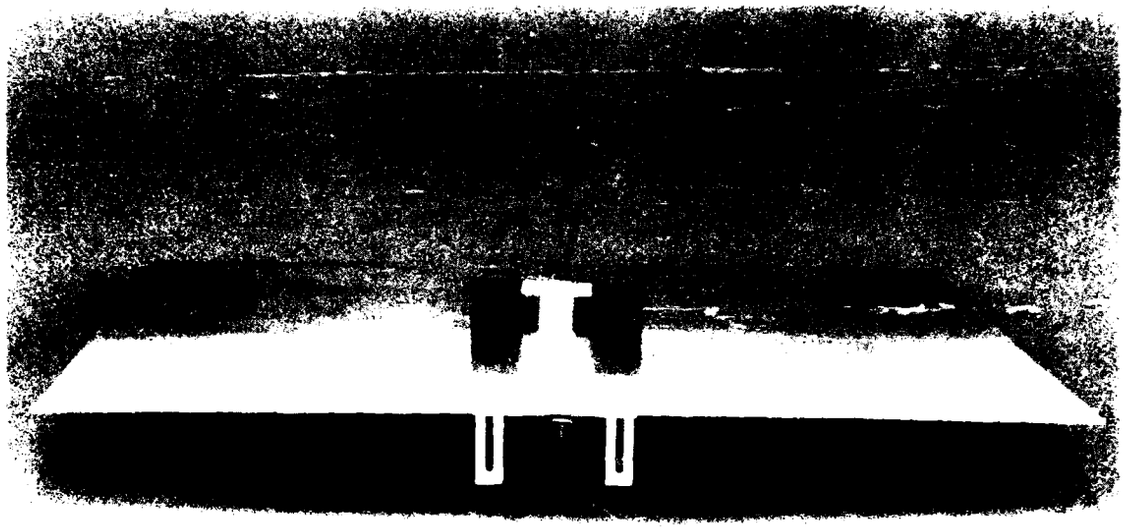

Figure 9. Folded Dipole over a Ground Plane

3.2 VSWR Measurements

Figures 10 and 11 show the measured and theoretical results of the two dipoles that were fabricated. SWR measurements were made on a HP8408A Automatic Network Analyzer with dipoles mounted $\lambda_o/4$ above the ground plane. As seen in Figure 10, the bandwidth of the dipole fabricated on the $\varepsilon_r = 4.4$ material was 36 percent, about 5 percent higher than for the $\varepsilon_r = 2.54$ material. Also note the characteristic double resonance of the dipole/balun configuration. Both the depth of the resonance, and the frequency at which the resonance occurs can be changed slightly if necessary by trimming the length of the two stubs (that is the slot length and/or the open end length) that make up the balun. When the balun is trimmed in this manner, one resonance will shift in frequency, as the other resonance remains relatively constant. Both resonances will however, change in depth. The resonance that remains relatively constant as the balun is trimmed, indicates the resonant frequency of the dipole, as the tuning stubs mainly affect only the second resonance. Having the capability of tuning the dipole/balun after it has been fabricated should prove to be very attractive, in that fabrication or material errors that are introduced into the design can be compensated for by trimming the two stubs. It is suggested that the slot length and open-end length be etched slightly longer than expected in a first run dipole/balun, since it is much easier to remove copper from the open or add tape to the slot, than to remove copper from the slot or add tape to the open.

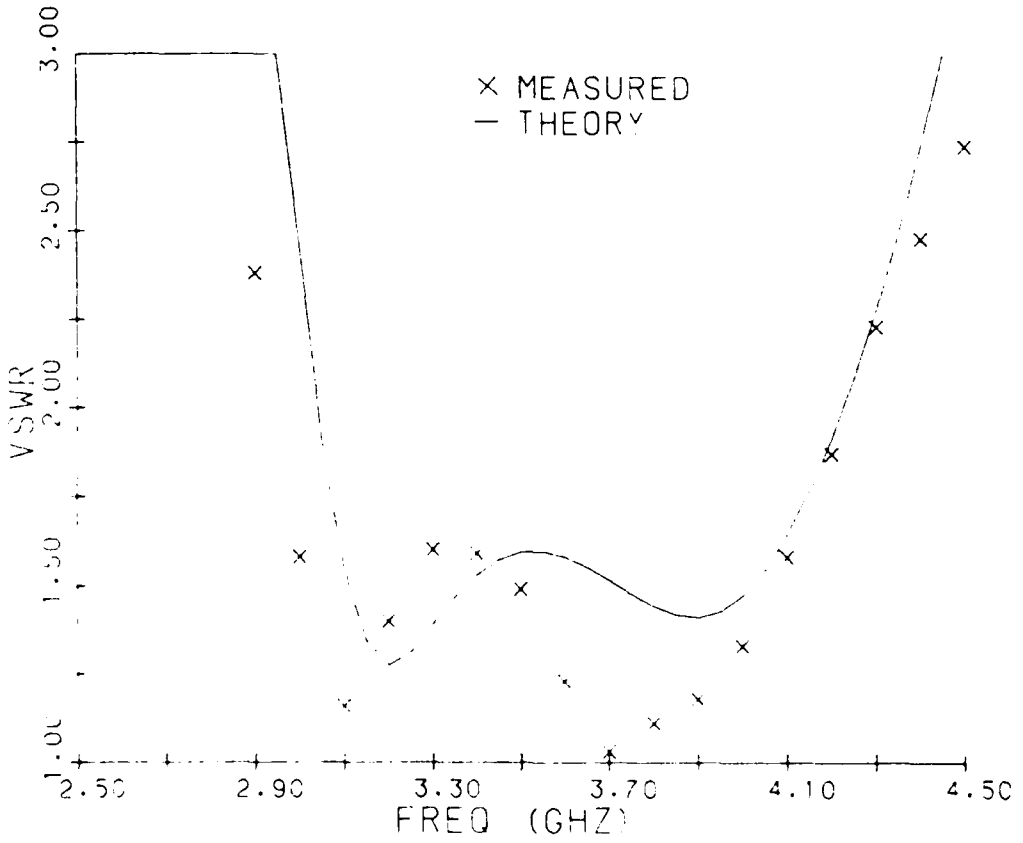

Figure 10. Measured and Theoretical VSWR, 4.4 Material

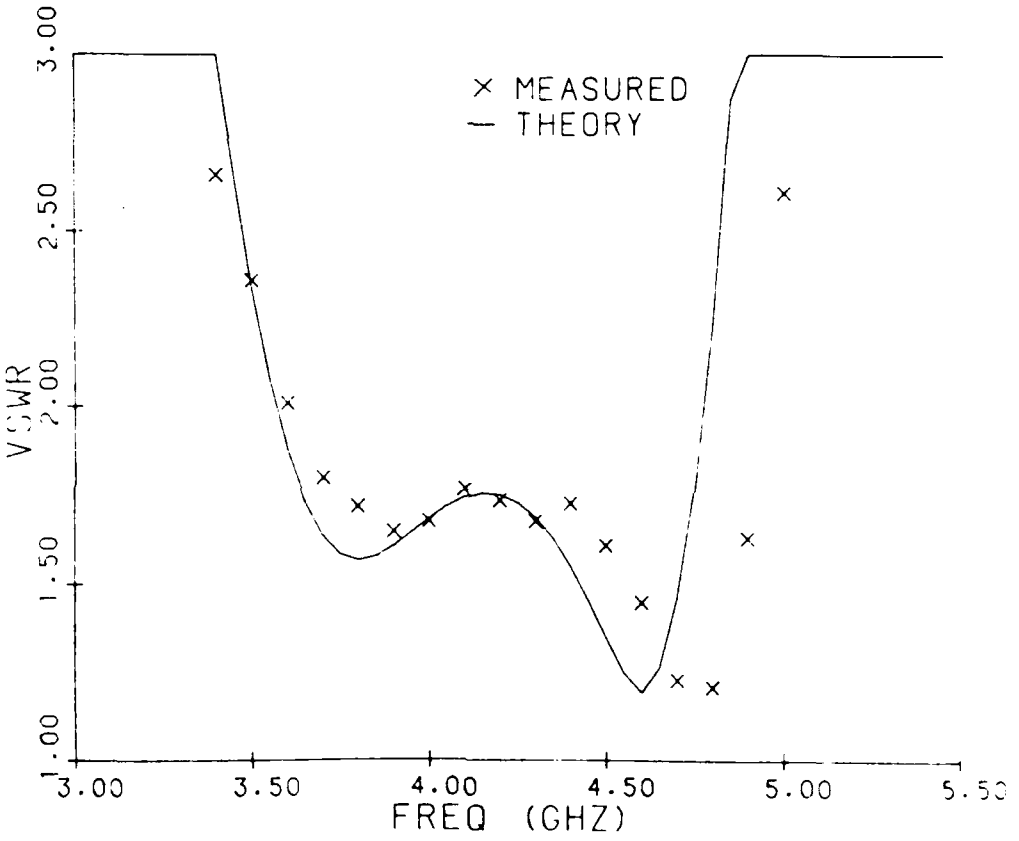

Figure 11. Measured and Theoretical VSWR, 2.54 Material

3.3 Antenna Patterns

Measured E- and H- plane patterns of the two dipoles are shown in Figures 12 and 13. It was noted during the pattern measurements that good electrical contact is required between the aluminum ground plane and the substrate's ground plane. Patterns will be moderately degraded if this precaution is not adhered to. Also, absorber was used to enclose hardware located behind the aluminum ground plane. This eliminated any contributions to the antenna pattern due to spurious radiation emitted by the feed line and the coax-to-microstrip transition.

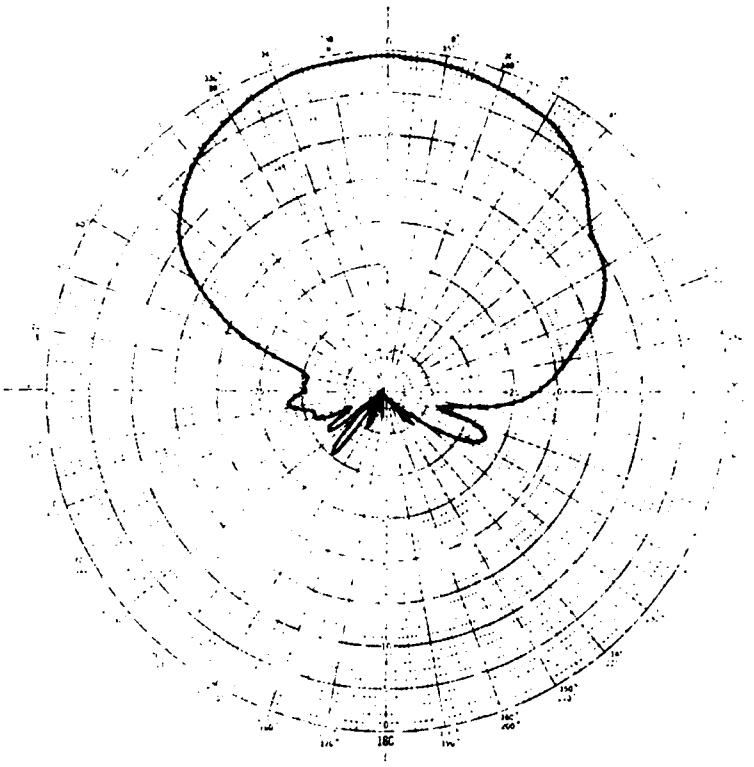

(a) E-Plane

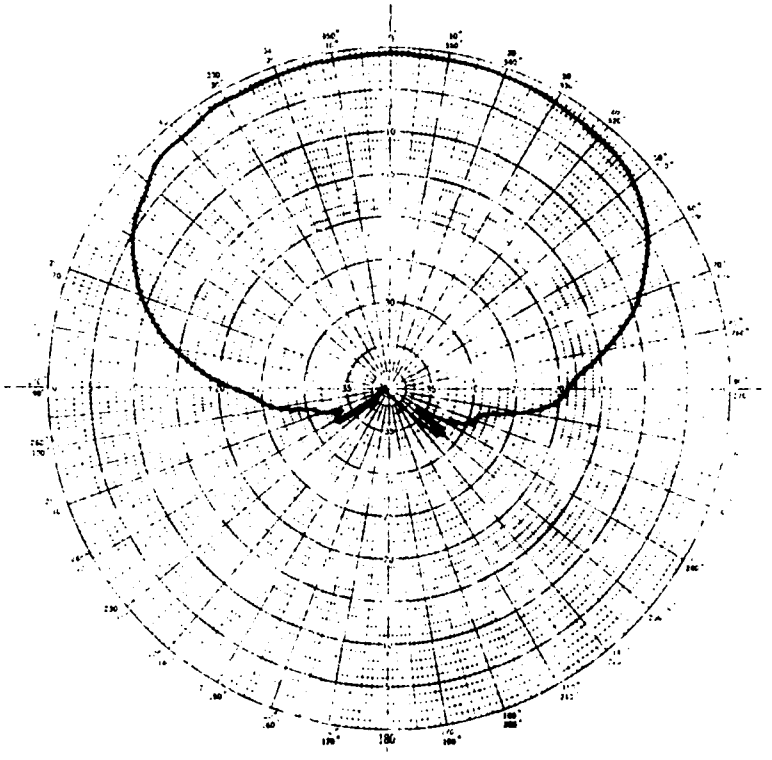

(b) H-Plane

Figure 12. Antenna Patterns, 4.4 Material, 3.7 GHz

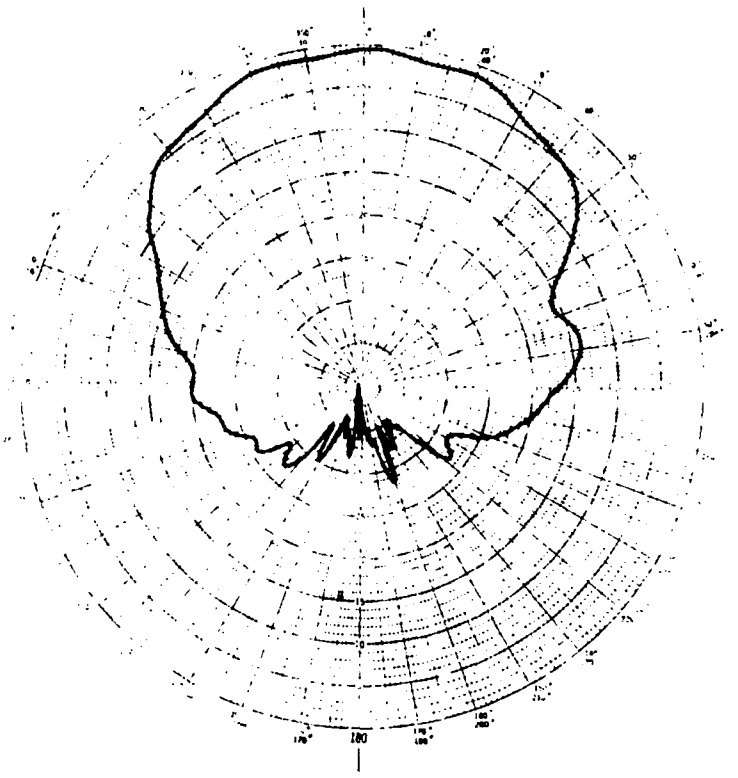

(a) E-Plane

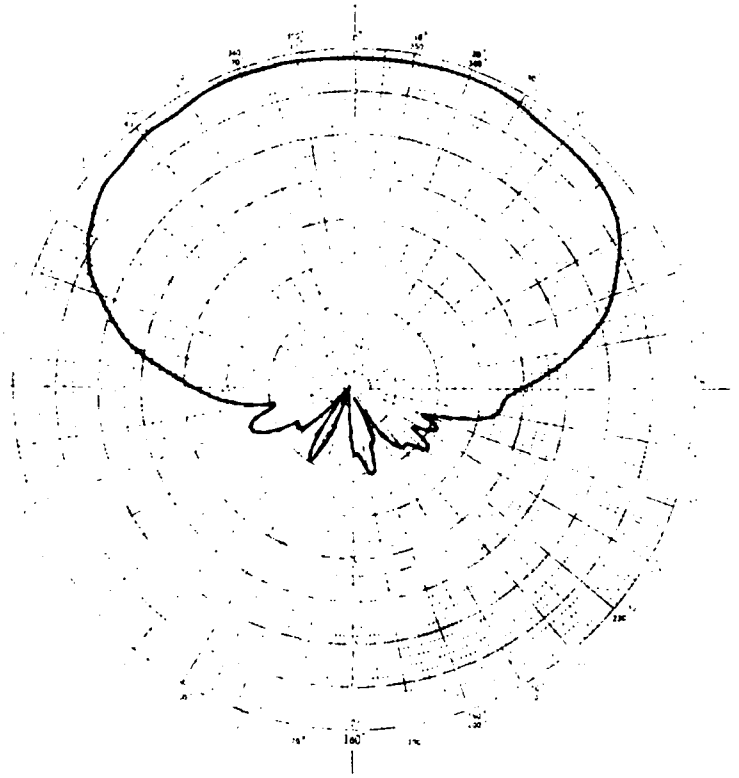

(b) H-Plane

Figure 13. Antenna Patterns, 2.54 Material, 4.2 GHz

Next, patterns were taken at several frequencies over the operating band to determine any frequency dependence of the patterns. The results are shown in Figures 14 through 17. Comparing Figure 16b to Figure 17b, it can be seen that the antenna patterns became slightly broader as frequency is increased from 3.5 to 5.0 GHz. This is due to the fact that the electrical distance between the dipole and ground plane increases as frequency is increased. In fact, if the frequency is increased such that the distance of the dipole above the ground plane reaches $\lambda_o/2$ a null will appear in the pattern at broadside. It is also interesting to compare antenna patterns of the dipole fabricated on the ε_r= 4.4 material, with the antenna patterns of the dipole fabricated on the ε_r= 2.54 material taken at the same frequency. Comparing Figure 13b to Figure 15b we see that the H-plane patterns of the two dipoles are virtually identical. The E-plane patterns (Figures 13a and 15a) are also very close inside the ±60 degree region, but are very much different outside this region. It is suspected that radiation from the open ended microstrip line is much more pronounced on the 2.54 material and therefore the degradation in the antenna pattern. The cross-polarization patterns of the dipole fabricated on the 2.54 material are also much worse than those of the 4.4 material and could be a significant contributor to the antenna pattern outside the ±60 degree region.

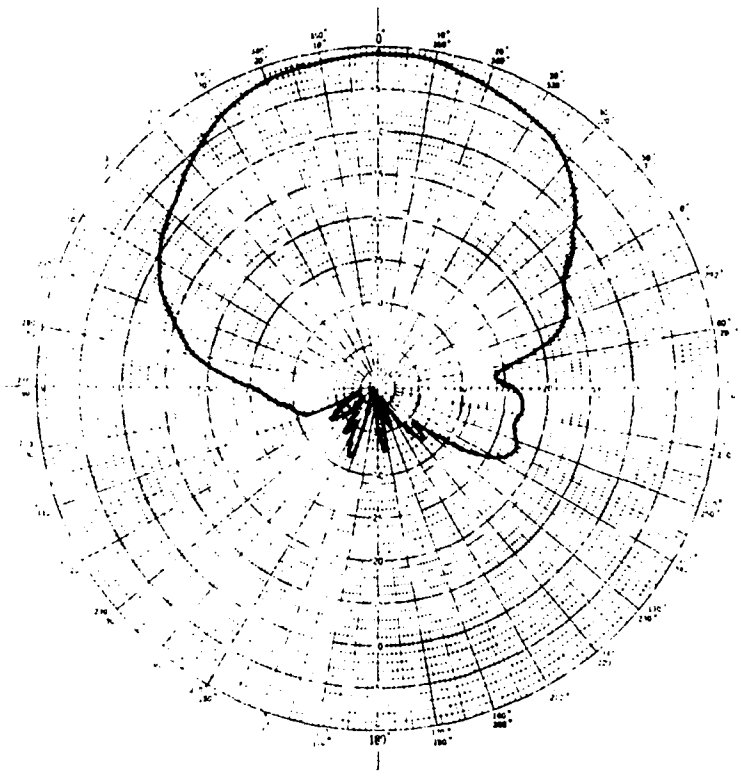

(a) E-Plane

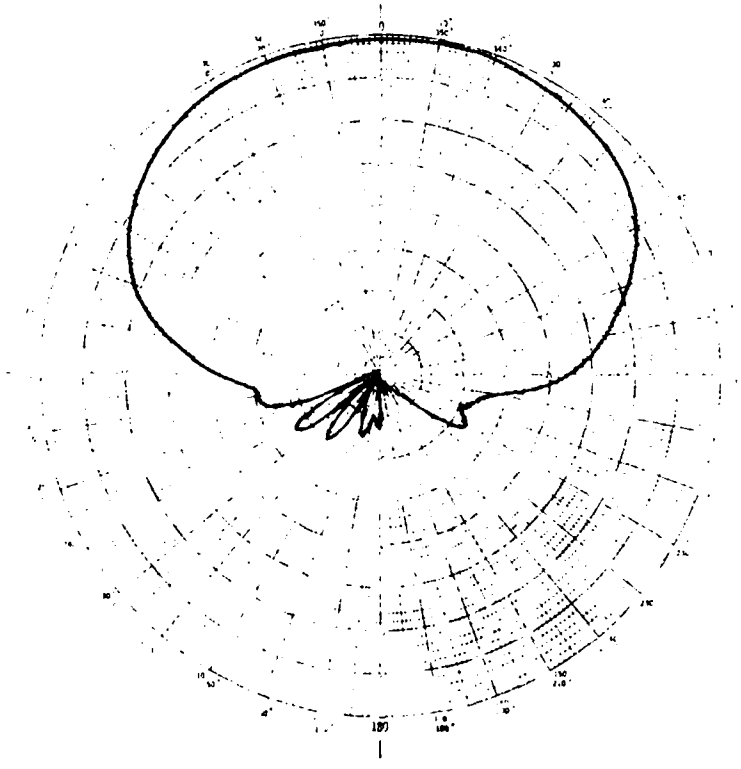

(b) H-Plane

Figure 14. Antenna Patterns, 4.4 Material, 3.1 GHz

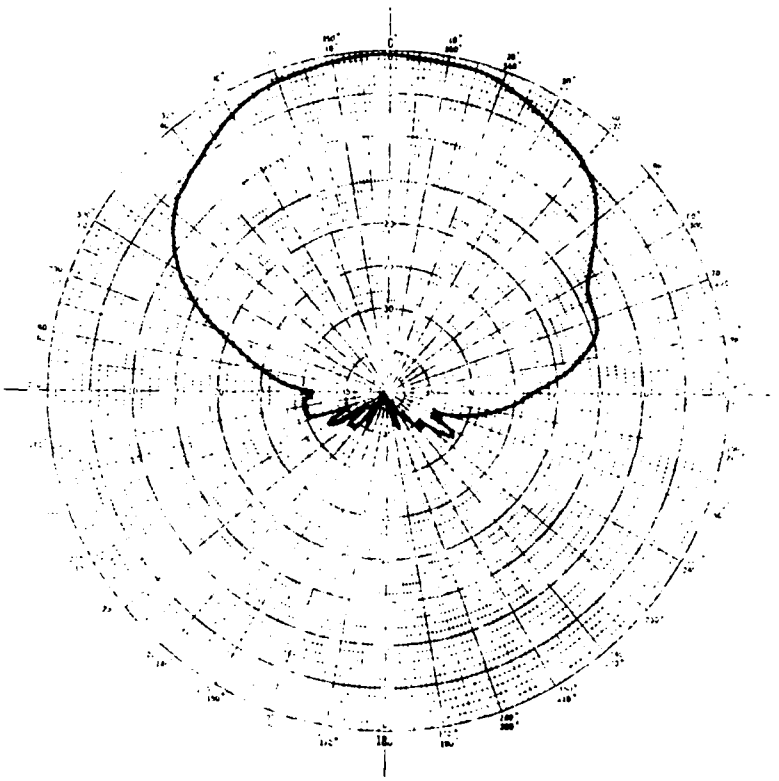

(a) E-Plane

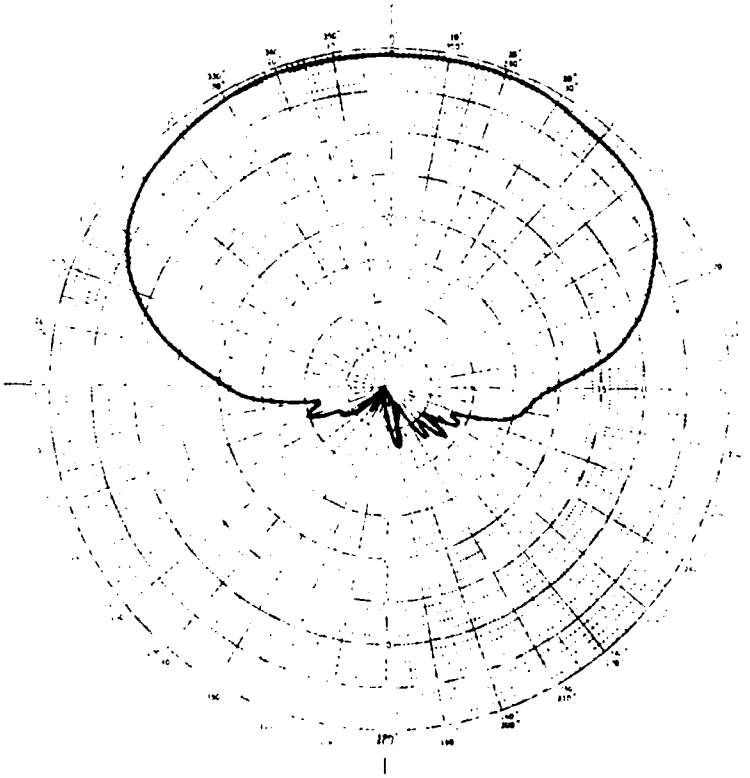

(b) H-Plane

Figure 15. Antenna Patterns, 4.4 Material, 4.2 GHz

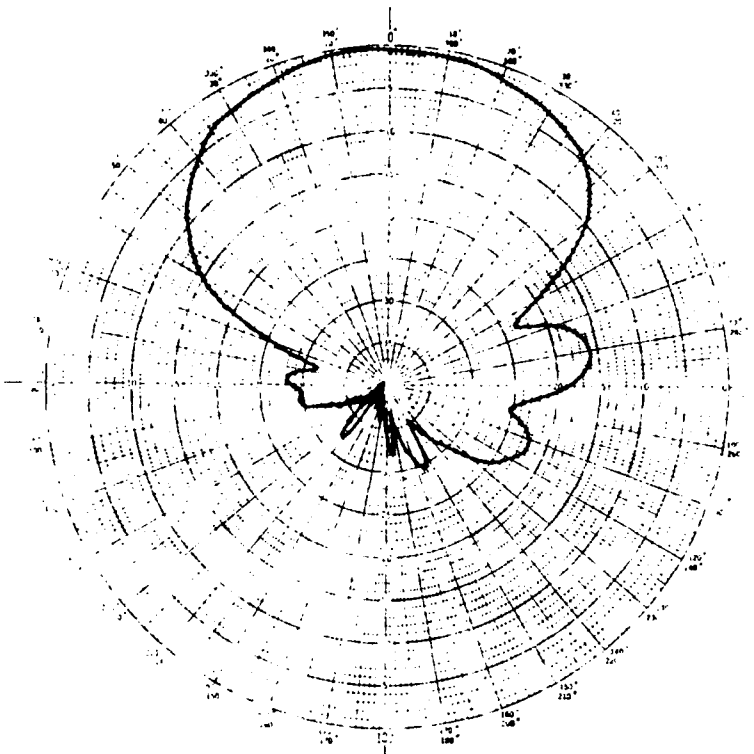

(a) E-Plane

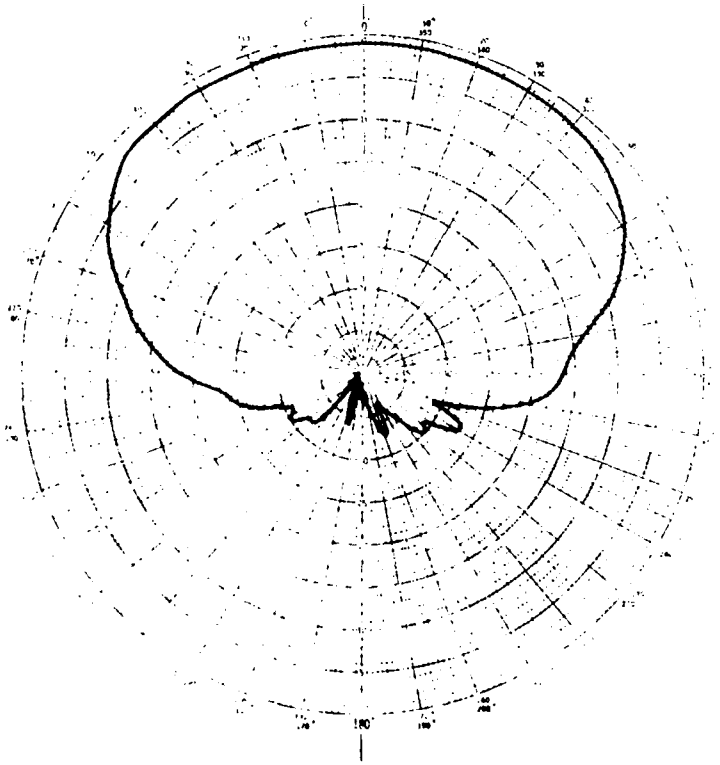

(b) H-Plane

Figure 16. Antenna Patterns, 2.54 Material, 3.5 GHz

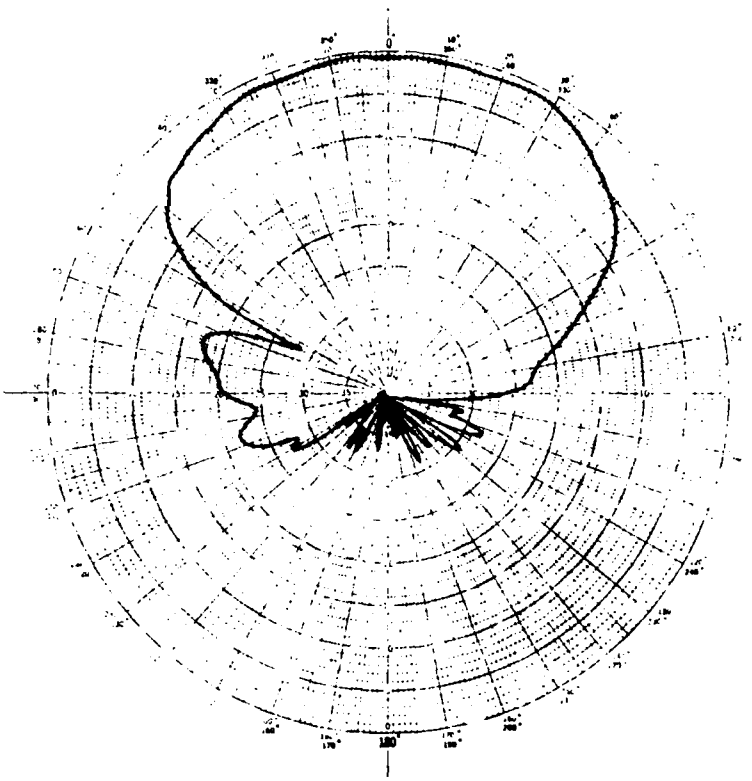

(a) E-Plane

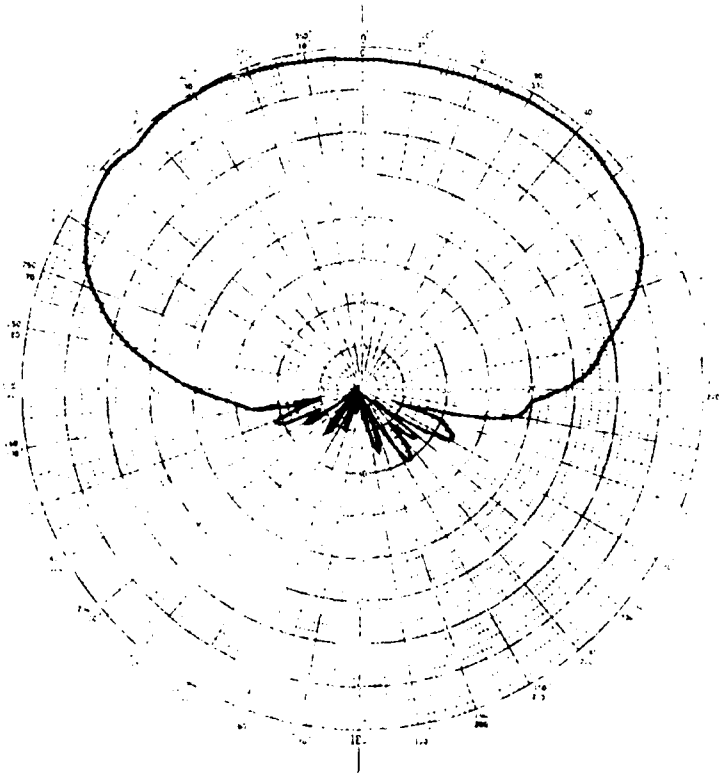

(b) H-Plane

Figure 17. Antenna Patterns, 2.54 Material, 5.0 GHz

Cross-polarization patterns are shown in Figures 18 through 23. All cross-polarization patterns were measured relative to the co-polarization. For both substrates, the trend here was two lobes approximately 11-20 dB down to occur at ±70 degrees from broadside in the H-plane cross-polarization patterns, and a single lobe approximately 15-21 dB down to occur near broadside in the E-plane cross-polarization patterns. The cross-polarization patterns taken of the dipole fabricated on the 4.4 material averaged about 5 dB below those taken of the dipole on the 2.54 material. Since similar cross-polarization patterns occur with the conventional dipole/balun configuration[14], it might be concluded that the cross-polarization patterns are primarily a function of the balun (that is the open ended microstrip line) rather than the dipole element itself.

[14] Mullinix, D.A. and Proudfoot, P.M. (1988) Printed Circuit Antenna Designs, *Proc. Antenna Applications Symposium*, Champaign-Urbana, IL.

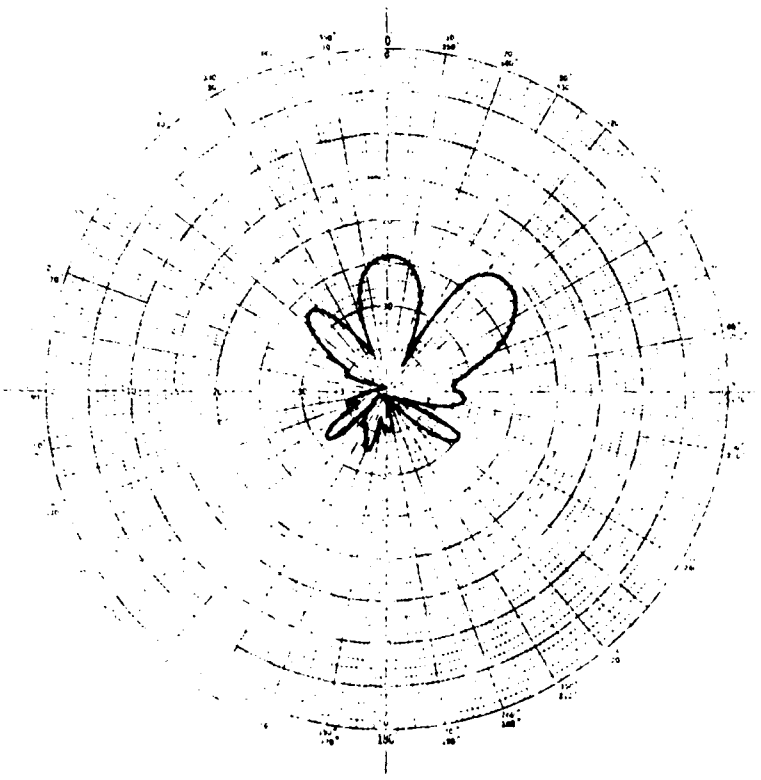

(a) E-Plane

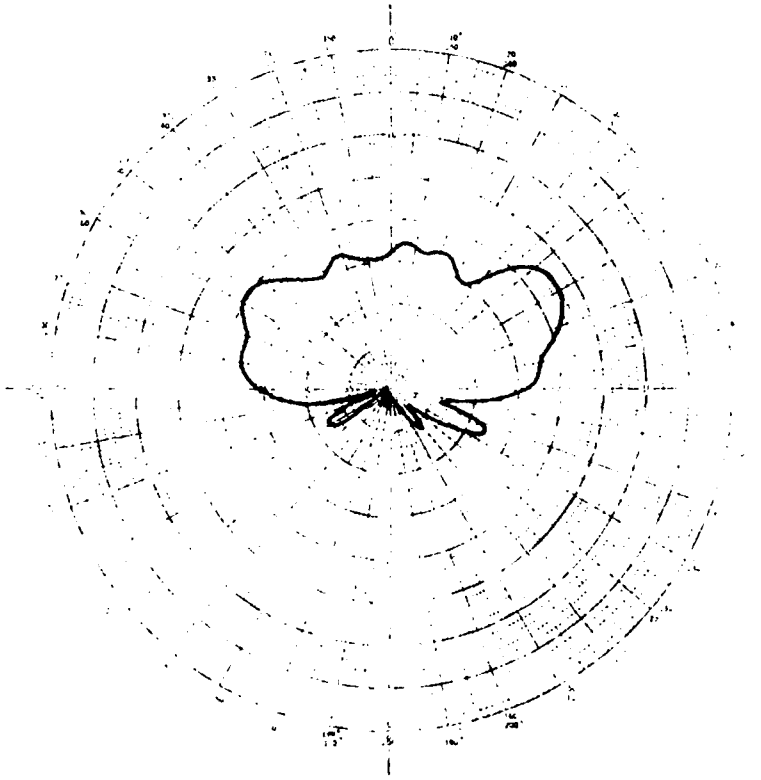

(b) H-Plane

Figure 18. Cross-Polarized Patterns, 4.4 Material, 3.1 GHz

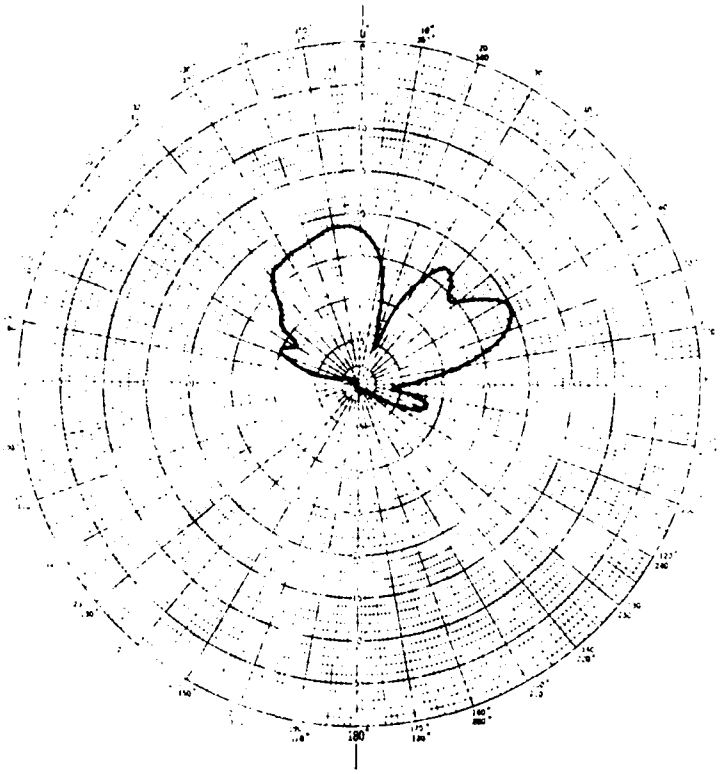

(a) E-Plane

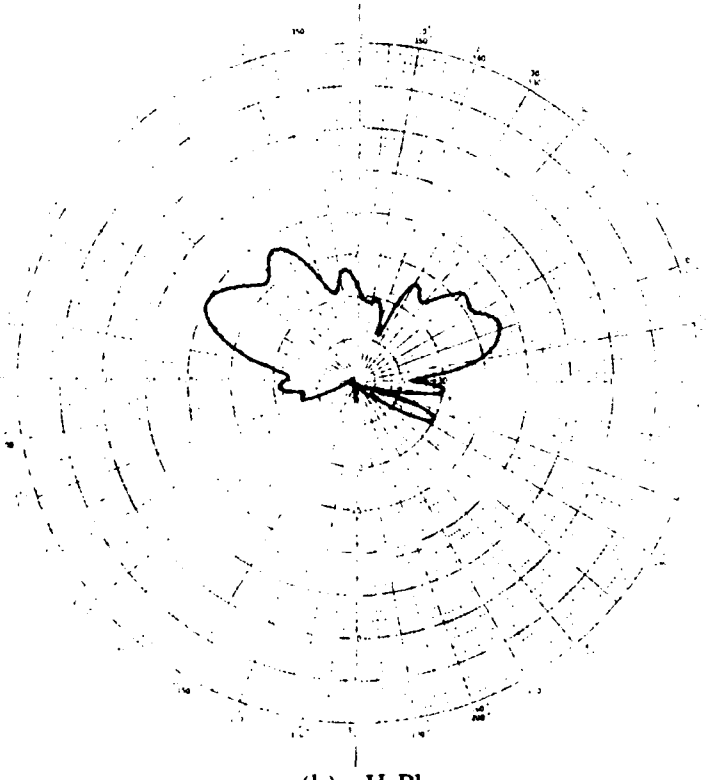

(b) H-Plane

Figure 19. Cross-Polarized Patterns, 4.4 Material, 3.7 GHz

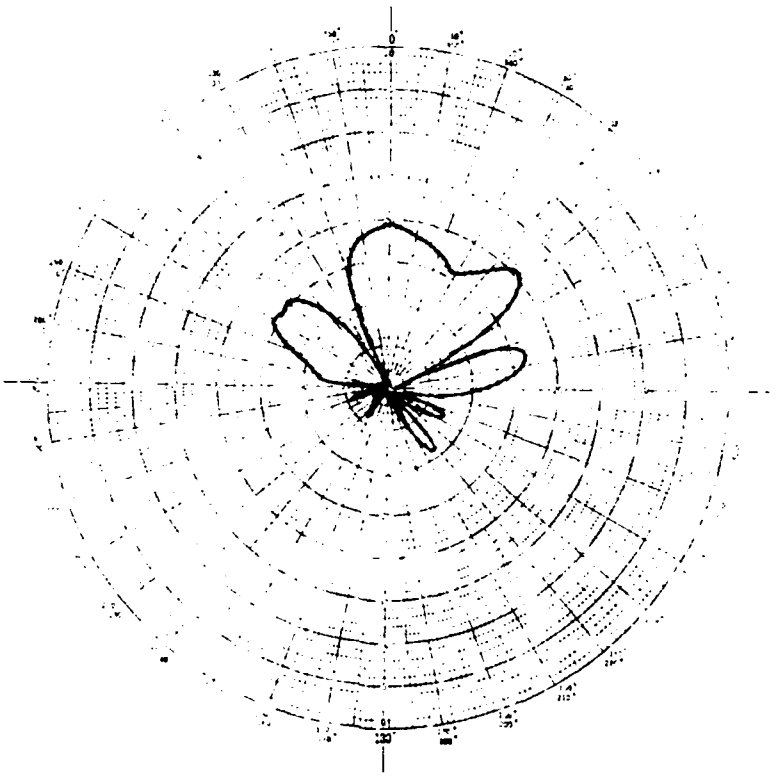

(a) E-Plane

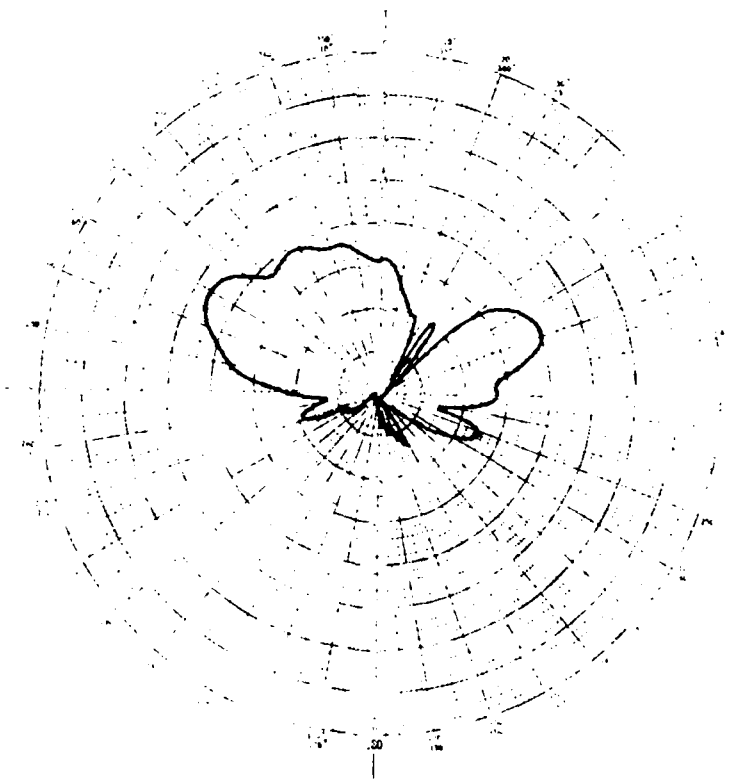

(b) H-Plane

Figure 20. Cross-Polarized Patterns, 4.4 Material 4.2 GHz

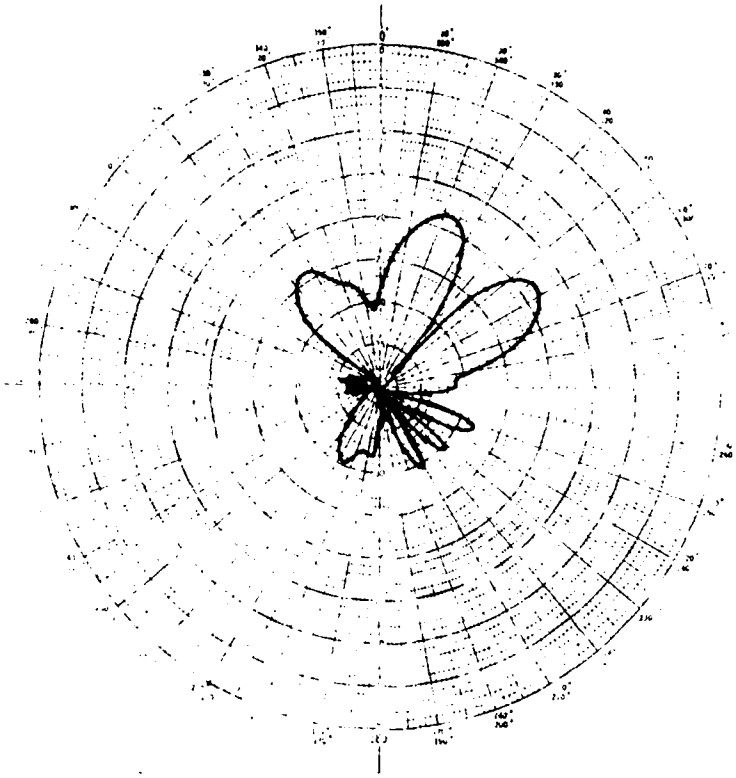

(a) E-Plane

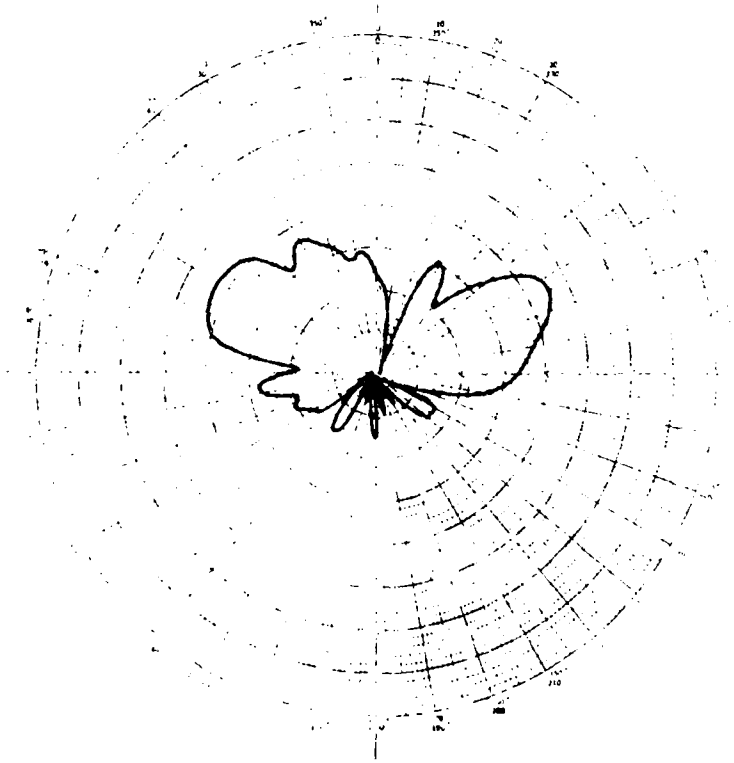

(b) H-Plane

Figure 21. Cross-Polarized Patterns, 2.54 Material 3.5 GHz

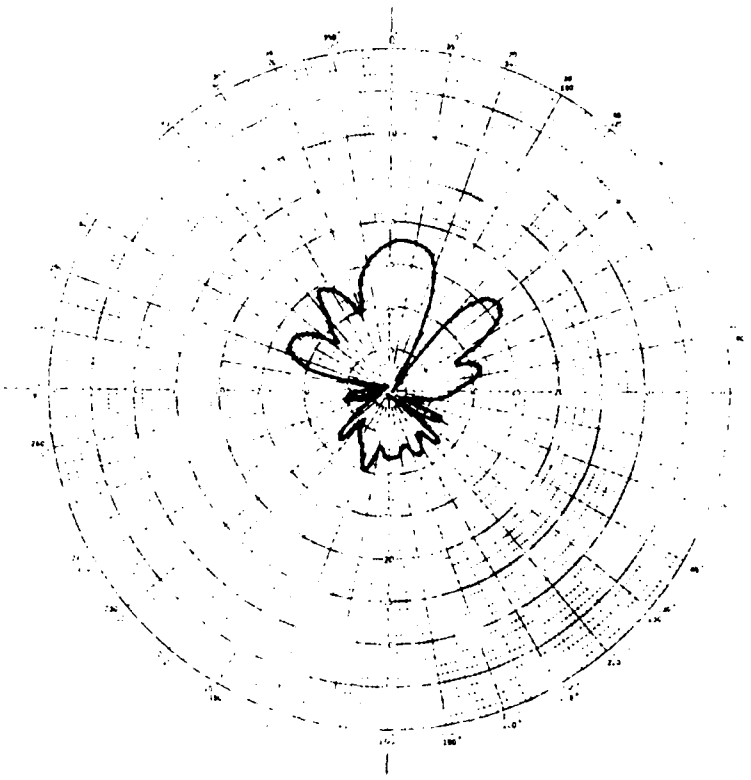

(a) E-Plane

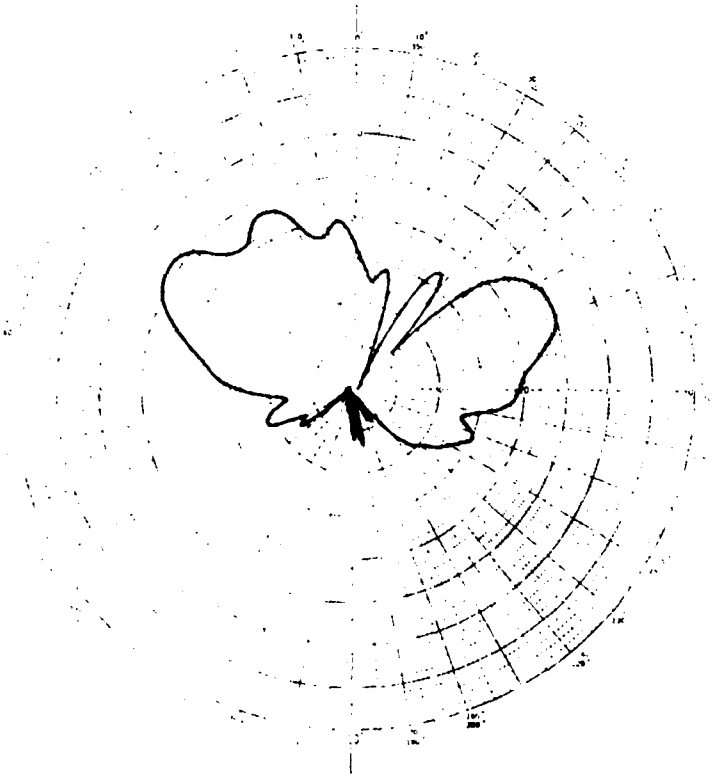

(b) H-Plane

Figure 22. Cross-Polarized Patterns, 2.54 Material, 4.2 GHz

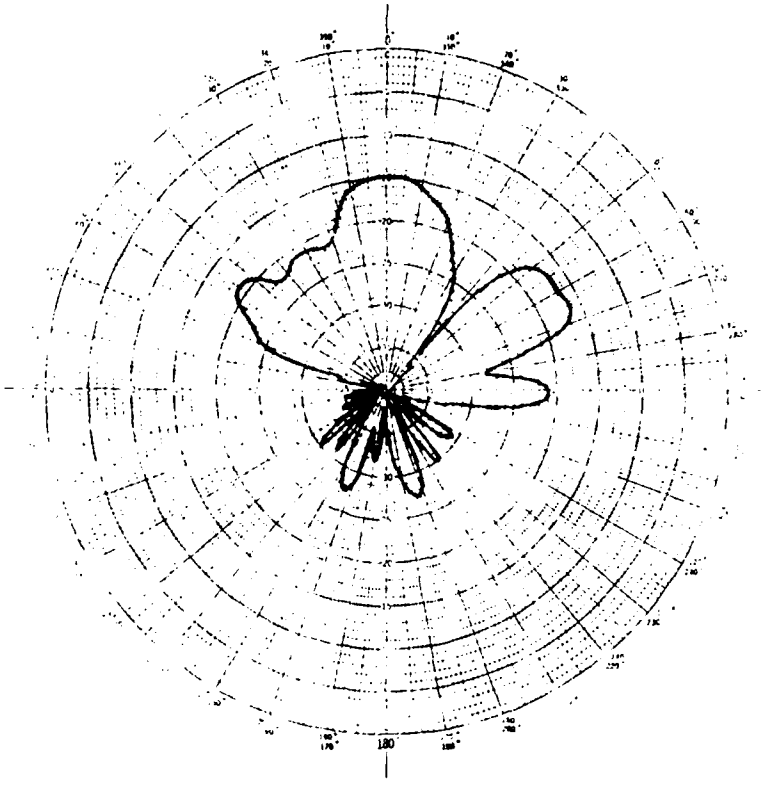

(a) E-Plane

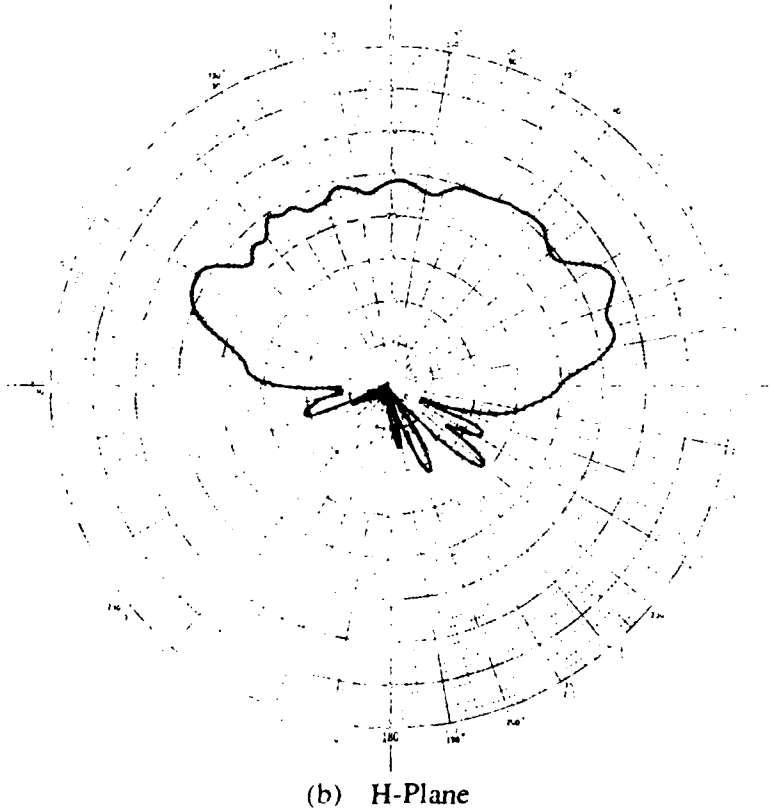

(b) H-Plane

Figure 23. Cross-Polarized Patterns, 2.54 Material, 5.0 GHz

4. CONCLUSION

The broad-band operation of a printed circuit folded dipole with integrated balun was demonstrated. Measured bandwidths of 31-36 percent were obtained and bandwidths of 40 percent should be possible. Antenna patterns show slight frequency dependence. Cross polarization could become a problem when radiation from the open ended microstrip line is excessive. Simple, easy-to-use, design equations were presented that lend themselves nicely to computer-aided design. This device should find many applications as a broad-band, low-cost and light-weight array element, capable of tight interelement spacings.

References

1. Lampe, R.L. (1985) Design formulas for an asymmetric coplanar strip folded dipole, *IEEE Trans. Antennas Propagat.* **AP-33**:1023-1031.

2. Herper, J.C., Hessel, A., and Tomasic, B. (1985) Element pattern of an axial dipole in a cylindrical phased array, Part II, *IEEE Trans. Antennas Propagat.* **AP-33**:273-278.

3. Edward, B. and Rees, D. (1987) A broadband printed dipole with integrated balun, *Microwave J.* **30**:339-344.

4. Roberts, W.K. (1957) A new wide-band balun, *Proc. IRE* **45**:1628-1631.

5. Bawer, R. and Wolfe, J.J. (1960) A printed circuit balun for use with spiral antennas, *IRE Trans. on Microwave Theory Tech.* **MTT-8**:319-325.

6. Gupta, K.C., Garg, R., and Chadha, R. (1981) *Computer Aided Design of Microwave Circuits*, Artech House, Dedham, MA.

7. McGrath, D.T., Mullinix, D.A., and Huck, K.D. (1986) *FORTRAN Subroutines for Design of Printed Circuit Antennas*, RADC-TM-86-08, ADB107263L.

8. Akhtarzad, S., Rowbotham, T.R., and Johns, P.B. (1975) The design of coupled microstrip lines, *IEEE Trans. Microwave Theory Tech.* MTT-23:486-492.

9. Kirschning, M. and Jansen, R.H. (1984) Accurate wide-range design equations for the frequency dependent characteristics of parallel coupled microstrip lines, *IEEE Trans. Microwave Theory Tech.* **MTT-32**:83-90.

10. Johnson, R.C. and Jasik, H. (1984) *Antenna Engineering Handbook*, McGraw-Hill, New York.

11. Hilberg, W. (1969) From approximations to exact relations for characteristic impedances, *IEEE Trans. Microwave Theory Tech.* MTT-17:259-265.

12. Lo, Y.T. (1953) A note on the cylindrical antenna of noncircular cross-section, *J. Appl. Phys.* Vol 24:1338-1339.

13. Balanis, C.A. (1982) *Antenna Theory*, Harper and Row, New York, pp.319-321.

14. Mullinix, D.A. and Proudfoot, P.M. (1988) Printed circuit antenna designs, *Proc. Antenna Applications Symposium*, Champaign-Urbana, IL.

MISSION
of
Rome Air Development Center

RADC plans and executes research, development, test and selected acquisition programs in support of Command, Control, Communications and Intelligence (C^3I) activities. Technical and engineering support within areas of competence is provided to ESD Program Offices (POs) and other ESD elements to perform effective acquisition of C^3I systems. The areas of technical competence include communications, command and control, battle management information processing, surveillance sensors, intelligence data collection and handling, solid state sciences, electromagnetics, and propagation, and electronic reliability/maintainability and compatibility.